PHYSICAL REVIEW B **105**, L180202 (2022)

Letter

Quantum boomerang effect in systems without time-reversal symmetry

Jakub Janarek,[1,2,*] Benoît Grémaud,[3,†] Jakub Zakrzewski,[2,4,‡] and Dominique Delande[1,§]

[1]*Laboratoire Kastler Brossel, Sorbonne Université, CNRS, ENS-PSL Research University, Collège de France, 4 Place Jussieu, 75005 Paris, France*

[2]*Instytut Fizyki Teoretycznej, Uniwersytet Jagielloński, Łojasiewicza 11, PL-30-348 Kraków, Poland*

[3]*Aix-Marseille Université, Université de Toulon, CNRS, CPT, Marseille, France*

[4]*Mark Kac Complex Systems Research Center, Uniwersytet Jagielloński, Kraków, Poland*

(Received 25 March 2022; accepted 17 May 2022; published 26 May 2022)

In an Anderson localized system, a quantum particle with a nonzero initial velocity returns, on average, to its origin. This recently discovered behavior is known as the quantum boomerang effect. Time-reversal invariance was initially thought to be a necessary condition for the existence of this phenomenon. We theoretically analyze the impact of the symmetry breaking on the phenomenon using a one-dimensional system with a spin-orbit coupling and show that the time-reversal invariance is not necessary for the boomerang effect to occur. We explain this behavior giving sufficient symmetry conditions for the boomerang effect to occur when time-reversal symmetry is broken.

DOI: 10.1103/PhysRevB.105.L180202

Introduction. Anderson localization (AL), the inhibition of transport due to the destructive interference of partial waves [1], is one of the most important phenomena in disordered systems. AL was successfully observed in quantum systems [2–6], as well as for acoustic [7] and electromagnetic waves [8,9]. While several manifestations of AL were discussed over the years, an entirely new phenomenon was recently discovered—the quantum boomerang effect (QBE) [10]: The center of mass (CoM) of a quantum particle launched with a nonzero velocity in a disordered potential returns, on average, to its initial position when AL is present. In stark contrast, a classical particle will end, on average, at a finite distance (one transport mean free path) from its initial position. The phenomenon appears as a smoking gun of AL and occurs in one- and higher-dimensional systems [10], including pseudorandom potentials and the localization in momentum space as exhibited by a kicked rotor [11]. Very recently, an experimental observation of the QBE was reported for the kicked rotor [12].

Consider a one-dimensional Hamiltonian $H = p^2/2m + V(x)$, where $V(x)$ is a disordered potential, e.g., a Gaussian uncorrelated disorder [10]. For a wave packet with some initial velocity $\psi_0(x) = \mathcal{N}\exp(-x^2/2\sigma^2 + ik_0x)$, the temporal evolution of the CoM is computed using $\langle x(t)\rangle = \int x\,\overline{|\psi(x,t)|^2}dx$, where $\overline{(\cdots)}$ denotes the average over disorder realizations. The QBE assures that the CoM returns to the origin, $\langle x(t=\infty)\rangle = 0$. Until now, the existence of the QBE has been supported by time-reversal invariance (TRI) arguments. In our work, we study the QBE in a system which breaks TRI. We show that the QBE may exist in such a situation. First, we show it on a simple example, both numerically and using the perturbative Berezinskii expansion. Later we formulate the sufficient conditions for QBE to occur when TRI is broken.

The model. We consider a one-dimensional single-particle system with spin-orbit (SO) coupling and Zeeman splitting as the minimum ingredient to break TRI and all antiunitary symmetries. For this purpose we use the following well-known Hamiltonian [13,14]:

$$H_0 = \frac{\hat{p}^2}{2m} + \gamma\hat{p}\sigma_z + \frac{\hbar\delta}{2}\sigma_z + \frac{\hbar\Omega}{2}\sigma_x, \quad (1)$$

where σ_i are the standard Pauli matrices. The Hilbert space is spanned by two-component complex-valued spinors. A specific experimental realization has been presented in [13,14], using a Raman coupling between two atomic states. γ is the strength of the SO coupling, Ω is the Rabi frequency of the Raman coupling, and δ its detuning. Due to translational invariance of H_0 the eigenstates can be labeled by wave numbers k. The spectrum of the Hamiltonian H_0 consists of two bands, $E_\pm(k) = \hbar^2k^2/2m \pm \hbar/2\sqrt{(2\gamma k+\delta)^2+\Omega^2}$, shown in Fig. 1. In the numerical simulations we assume $\hbar = 1$ and $m = 1$. Every dimensional quantity is expressed through a chosen unit of length a, i.e., energies are in units of $\hbar m^{-1}a^{-2}$, times are in units of $\hbar^{-1}ma^2$, disorder strength η in units of $\hbar^2m^{-2}a^{-3}$, velocities in units of $\hbar m^{-1}a^{-1}$, wave numbers in units of a^{-1}, etc.

To study the QBE we add to the Hamiltonian a disordered potential, $H = H_0 + V(x)$, similarly to [15]. For the disorder we choose a Gaussian uncorrelated disorder: $\overline{V(x)} = 0$, $\overline{V(x)V(x')} = \eta\delta(x-x')$, where η denotes the disorder strength. The disorder is the same for both spin components.

Condition for QBE. Can we observe the QBE for our model? In [10] it was proved that time-reversal invariance of the Hamiltonian was a sufficient condition for the QBE to exist [16].

*jakub.janarek@uj.edu.pl
†benoit.gremaud@cpt.univ-mrs.fr
‡jakub.zakrzewski@uj.edu.pl
§dominique.delande@lkb.upmc.fr

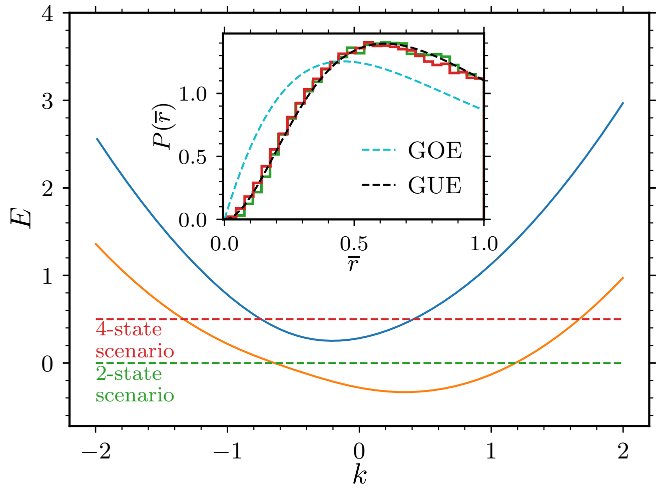

FIG. 1. Spectrum of the Hamiltonian (1) computed for $\gamma = 0.4$ and $\delta = \Omega = 0.4$. Depending on the choice of the parameters, there are up to four possible eigenstates at a given energy with different velocities. The green (red) dashed line represents an example of a two-state (four-state) scenario. The inset displays the distributions of gap ratio $P(\bar{r})$ calculated around $E = 0$ and $E = 0.5$. The dashed lines are theoretical predictions for the GOE and GUE symmetry classes.

For a spin-1/2 particle, the standard antiunitary time-reversal operator is $T = i\sigma_y K$, where K denotes the the time-reversal operator for a spinless particle that is complex conjugation in configuration space [17] such that $x \to -x, t \to -t, p \to -p, K\psi(x) = \psi^*(x)$. If $\gamma \neq 0$, the disordered Hamiltonian H breaks time-reversal invariance $THT^{-1} \neq H$. This is however not the end of the story. As discussed in [11,12], there are cases—such as the kicked rotor—where another antiunitary symmetry, e.g., the product TP of the conventional time-reversal T, with spatial parity P, such that $x \to -x, t \to t, p \to -p$, is sufficient to imply the QBE.

In our model we have found that, for $\delta = 0$, the Hamiltonian is invariant under the generalized antiunitary operator $\mathcal{T} = i\sigma_z K$. The disorder $V(x)$ breaks all the possible spatial symmetries. As a consequence, when δ, Ω, γ are all nonzero, any generalized time-reversal symmetry is broken, and the Hamiltonian belongs to the unitary symmetry class represented by Gaussian unitary ensemble (GUE) [instead of the Gaussian orthogonal ensemble (GOE) appropriate for PT or $\mathcal{T}$ symmetric case] [17]. As a numerical evidence, the inset in Fig. 1 displays distributions of gap ratio $\bar{r} = \min(\delta_n/\delta_{n-1}, \delta_{n-1}/\delta_n)$, where δ_n is the spacing between neighboring energy levels [18,19]. The figure shows a very good agreement of numerical data with the theoretical prediction for the GUE [19], proving that all antiunitary symmetries are broken.

Weak disorder couples disorder-free eigenstates with the same energy, but different momenta and spin states. We first study the two-state scenario, see Fig. 1. There are two momenta $k_\pm$ and two corresponding spinors $|\chi_\pm\rangle$ such that $|k_\pm\rangle \otimes |\chi_\pm\rangle$ are eigenstates of the disorder-free Hamiltonian (1) with the same energy E_0. Note that $k_- \neq -k_+$, where the associated velocities $v_\pm = \frac{1}{\hbar}\frac{dE(k_\pm)}{dk}$ are not opposite and that the spin states $|\chi_\pm\rangle$ are not orthogonal.

For the initial wave packet, we use either one of the two states $|\Psi_0^\pm\rangle = |\psi_0^\pm\rangle \otimes |\chi_\pm\rangle$, where $\psi_0^\pm(x) = \mathcal{N}\exp(-x^2/2\sigma^2 + ik_\pm x)$, $\mathcal{N}$ is a normalization constant. We distinguish results calculated for the two initial states by denoting them $\langle x_\pm \rangle$. In our simulations we have used $\sigma = 50$. The states $|\Psi_0^\pm\rangle$ are not exact eigenstates of H_0, they are approximations to monochromatic waves. However, based on the results of [10,20], we can safely assume that, as long as the initial state does not contain too many momentum components and disorder is weak, the results are essentially independent of σ. During the temporal evolution, only the two degenerate states are coupled by the weak disorder. The wave packet can thus be written as $|\psi(t)\rangle = |\psi_+(t)\rangle \otimes |\chi_+\rangle + |\psi_-(t)\rangle \otimes |\chi_-\rangle$, where $\psi_\pm(x,t) = \langle x|\psi_\pm(t)\rangle$ are the wave functions of the of the components propagating to the right (positive velocity, + sign) and the left (negative velocity, − sign). This allows us to compute the CoM as

$$\langle x(t)\rangle = \int x\left(\overline{|\psi_+(x,t)|^2} + \overline{|\psi_-(x,t)|^2}\right) dx\,. \tag{2}$$

Due to nonorthogonality of the spinors $|\chi\rangle_\pm$, there exists also an interference term $\psi_+(x,t)\psi_-(x,t) + \text{c.c.}$. This term, however, is quickly oscillating, hence its contribution can be neglected in Eq. (2).

There are in total four possible elastic scattering events: $+ \to +$, $+ \to -$, $- \to -$, and $- \to +$. The forward scattering events $+ \to +$, $- \to -$ do not affect the dynamics of the CoM. Hence, in further analysis we use only the two scattering events where the direction of motion is changed. The associated scattering mean free times $\tau_+ = \tau_{+\to-}$ and $\tau_- = \tau_{-\to+}$ can be computed at weak disorder from the Fermi golden rule or, equivalently, from the Born approximation [21,22]:

$$\frac{1}{\tau_+} = \frac{\eta\kappa}{\hbar^2|v_-|}, \quad \frac{1}{\tau_-} = \frac{\eta\kappa}{\hbar^2|v_+|}, \tag{3}$$

where $\kappa = |\langle\chi_+|\chi_-\rangle|^2$ is the spin-state overlap.

Classical solution. The classical problem is governed by coupled Boltzmann equations $\partial_t f_\pm = -v_\pm \partial_x f_\pm \mp f_+/\tau_+ \pm f_-/\tau_-$, where $f_\pm(x,t)$ are the population densities. The subscript $\pm$ denotes the direction of propagation. These Boltzmann equations are easily solved (see also Supplemental material [23]). We obtain:

$$\langle x_\pm \rangle^{\text{class.}} = v_\pm \tau[1 - \exp(-t/\tau)], \tag{4}$$

with $\tau = \tau_+\tau_-/(\tau_+ + \tau_-)$, a result very similar to the one obtained in the TRI case [10]. The particles, on average, travel a distance $|v_\pm|\tau$, then stop their evolution.

Quantum numerics. We take a system with $\gamma = 0.4$ and $\delta = \Omega = 0.4$. The solution is obtained in a box large enough for the wave packet not to touch the edges, $L = 10\,000$, with a sufficiently small discretization $\Delta x = 0.2$. The initial state's energy is chosen $E_0 = 0$, so that $k_- = -0.6453$ and $k_+ = 1.1850$. This also means that $\kappa = 0.505$ and the velocities are $v_- = -0.5340$ and $v_+ = 0.8014$. We have used disorder strength $\eta = 0.0049$, so that $\tau_- = 323.61$, $\tau_+ = 215.66$, $\tau = 129.42$, and the transport mean free path [23] is $\ell_t = \tau\sqrt{|v_-|v_+} = 84.67$. For the time propagation we have used the Chebyshev kernel method [24–27].

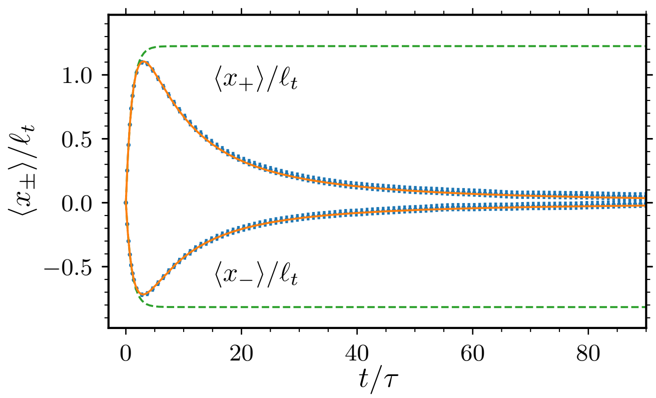

FIG. 2. Temporal evolution of the center of mass (2), for wave packets launched with a positive (upper curve) and negative (lower curve) velocity. The blue symbols (with error bars representing statistical errors, averaging over 40 960 disorder configuration) are the quasiexact numerical results. Even without time-reversal invariance, we observe the full quantum boomerang effect—the center of mass returns to the origin. The dashed lines present the classical solution (4) which does not return to the origin. The orange solid lines are the prediction of our fully quantum theory by Berezinskii.

The results of the simulations are presented in Fig. 2. Even though TRI is broken, we observe a *perfect* QBE. Similarly to the TRI case, the CoM returns to the origin after the initial ballistic motion. The figure also includes classical solutions (dashed lines) obtained using Boltzmann equations. For a very short time, the classical solutions agree with quantum simulations. Then Born approximation is sufficient to describe the quantum dynamics. However, from $t \approx 3\tau$, classical and quantum outcomes split, and the quantum particle returns to the origin.

The data displayed in Fig. 2 constitute a major result of this paper—presence of the full QBE without TRI. All previous studies of the boomerang effect [10–12,28] insisted on the importance of TRI (in addition to Anderson localization) for the boomerang effect. Here we can give a negative answer to the question whether TRI is a necessary condition for the QBE existence.

Diagrammatic approach. In addition to a purely numerical solution, Fig. 2 displays theoretical predictions, described below, which perfectly agree with numerics. We use an approach very similar to the one used for the TRI case in [10]: the Berezinskii diagrammatic technique [29]. The main difference with respect to earlier works [29–32] is that there are more different scattering vertices due to the lack of TRI in our case. The results are found as a Taylor series in powers of t for the CoM positions [23,33].

Here, for simplicity, we present solutions only for the positive initial velocity state. We obtain

$$\langle x_+(t)\rangle = v_+\tau\left[\frac{t}{\tau} - \frac{t^2}{2\tau^2} + \frac{t^3}{6\tau^3} - \frac{(1+\Delta(4+\Delta(8+\Delta(4+\Delta))))t^4}{24(1+\Delta)^4\tau^4}\right] + \mathcal{O}(t^5) \tag{5}$$

with $\Delta = |v_-/v_+|$.

This quantum solution agrees with the classical one up to third order:

$$\langle x_\pm(t)\rangle^{\text{class.}} = v_\pm\tau\left[\frac{t}{\tau} - \frac{t^2}{2\tau} + \frac{t^3}{6\tau^3} - \frac{t^4}{24\tau^4}\right] + \mathcal{O}(t^5), \tag{6}$$

similarly to the TRI boomerang [10]. Likewise, we find a finite radius of convergence for the series in Eq. (5), which seems to slightly depend on the value of Δ.

A significant difference between our solution and the TRI case is that $\langle x_\pm(t)\rangle$ is no longer universal. Starting from fourth order, all terms explicitly depend on Δ. Of course the TRI solution is fully recovered when $\Delta = 1$.

To describe the center of mass evolution for intermediate times, we use a Padé approximant [34] of the Taylor series. The long-time scaling should be similar to the TRI system, i.e., $\langle x(t \gg \tau)\rangle \propto t^{-2}$, as also supported by the numerical evidence. While, in the TRI case, there is a more accurate asymptotic expression [10]: $\langle x(t \gg \tau)\rangle \sim 64\ln(t/\tau)(\tau/t)^2$, the derivation is much more difficult when TRI is broken [33], so we only know for sure the leading t^{-2} behavior. Thus, we compute the CoM at any time as

$$\langle x_\pm(t)\rangle = \tau v_\pm\left(\frac{\tau}{t}\right)^2 \lim_{n\to\infty} R_n(t), \tag{7}$$

where $R_n(t)$ is a diagonal Padé approximant [34], whose coefficients are calculated from the short-time Taylor series, Eq. (5). To obtain high accuracy of the approximation, we use $n = 30$. There is however no visible difference with results obtained for lower n, e.g., $n = 20$.

We compare the theoretical results with the numerical data in Fig. 2. The agreement is outstanding. We have performed a slight adjustment of the scattering rates $1/\tau_\pm$, given in the weak disorder limit by Eq. (3) [23]. Indeed, higher order terms in the disorder strength η are known to exist [21], but they are small (of the order of 1%) and do not affect the structure of the Berezinskii method. Even without the adjustment, using the fully analytic expression (3), the agreement between the Berezinskii theory and the numerical results is excellent [23]. This shows that the boomerang effect not only survives the breaking of TRI, but also that the time evolution of the CoM can be computed theoretically.

The QBE also exists in the four-state scenario, when H_0 has four eigenstates with the same energy E_0, see Fig. 1. As shown in Fig. 3, after an initial fast departure from the origin, again the CoM returns to the origin exhibiting a perfect QBE. The dashed line is the classical solution of the coupled Boltzmann equations [23] which, amusingly, shows that the classical solution also reveals a tendency to return at short times, only then stopping at a nonzero distance from the origin. For this case, the diagrammatic approach, while feasible, would be very painful and is left for a possible future study.

Finally, we give an explanation of the observed QBE based on symmetry arguments. The product of the commuting parity operator P and spinless time-reversal operator T is such that $x \to -x, t \to -t, p \to p$ and does not touch the spin degree of freedom. It is an antiunitary operator squaring to +1; it is thus *not* a generalized time-reversal operator for the spin-1/2 system. It modifies the disordered Hamiltonian so that

$$PT\ H\ (PT)^{-1} = H_0 + V(-x) = \tilde{H} \neq H. \tag{8}$$

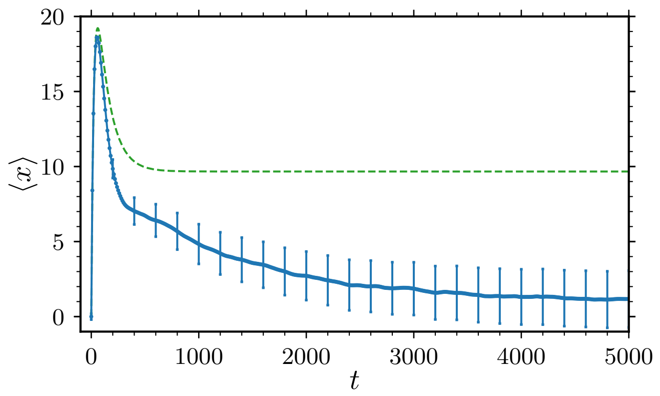

FIG. 3. Quantum boomerang effect in the four-state scenario of Fig. 1: $\gamma = 0.4$ and $\delta = \Omega = 0.4$, $E = 0.75$, and $\eta = 0.0225$ for a Gaussian state with initial momentum $k = 0.68$ and width $\sigma = 50$. The numerical calculation in blue shows that there is a full quantum boomerang effect at long time $\langle x(t \to \infty)\rangle = 0$. In contrast, the classical solution of the coupled Boltzmann equations indicate a finite displacement of the center of mass of the wave packet.

In an Anderson localized system, the infinite-time CoM position after evolving with H may be obtained using the diagonal approximation:

$$x^H(t=\infty) = \sum_i \langle\phi_i| x |\phi_i\rangle \, |\langle\phi_i|\psi_0\rangle|^2$$
$$= \sum_i \langle\phi_i| x |\phi_i\rangle \, |\langle\phi_i| TP\, PT\, |\psi_0\rangle|^2, \qquad (9)$$

where $\{|\phi_i\rangle\}$ is the eigenbasis of H and $|\psi_0\rangle$ is the initial state. The eigenstates of $\tilde{H}$ are $|\tilde{\phi}_i\rangle = PT\,|\phi_i\rangle$. We have $\langle\phi_i| x |\phi_i\rangle = -\langle\tilde{\phi}_i| x |\tilde{\phi}_i\rangle$. Inserting it in Eq. (9), we get

$$x^H(t=\infty) = -\sum_i \langle\tilde{\phi}_i| x |\tilde{\phi}_i\rangle \, |\langle\tilde{\phi}_i| PT\,|\psi_0\rangle|^2. \qquad (10)$$

Hence, if $PT\,|\psi_0\rangle = |\psi_0\rangle$ (which is the case for our initial Gaussian wave packets), then $x^H(t=\infty) = -x^{\tilde{H}}(t=\infty)$. For a single disorder realization, $x^H(t=\infty)$ is generically nonzero. However, because H and $\tilde{H}$ belong to the same statistical distribution of disorder with the same weight, after disorder averaging, we obtain

$$\langle x(t=\infty)\rangle = \overline{x^H(t=\infty)} = -\overline{x^{\tilde{H}}(t=\infty)} = 0, \qquad (11)$$

implying the full QBE.

The Hamiltonian H has no generalized TRI and is in the GUE symmetry class but still displays a full QBE, as exemplified in the inset of Fig. 1.

Summary. We have demonstrated the presence of the QBE in an exemplary spin-orbit system where all antiunitary symmetries—especially time-reversal invariance—are broken. We can give a sufficient condition for the appearance of the QBE in a general setting. The full QBE, i.e., $\langle x(t=\infty)\rangle = 0$, is present if there exists an unitary or antiunitary transformation U satisfying the following conditions: (i) the position operator is odd under the action of U: $UxU^{-1} = -x$, (ii) the disorder-free part of the Hamiltonian is symmetric under this transformation $UH_0U^{-1} = H_0$, (iii) the transformed disorder $\tilde{V} = UVU^{-1}$ is a valid disorder realization with the same weight, and (iv) and the initial state is symmetric under the transformation $U\,|\psi_0\rangle = |\psi_0\rangle$. For our Hamiltonian (1), such transformation is the product of the parity and spinless time-reversal operators $U = PT$.

By generalizing the Berezinskii diagrammatic approach to a system without TRI, we have computed the time evolution of the CoM in a quasianalytic way. The theoretical result is in perfect agreement with the numerical data for the spin-orbit coupled model. Although in our work we have studied a one-dimensional system, similarly to the TRI counterpart of the phenomenon, we believe that the QBE is also present in higher-dimensional unitary systems.

After the original submission of this work, the preprint [35] appeared which had a partial overlap with our finding and generalizes QBE to certain non-Hermitian systems.

Acknowledgments. We thank Tony Prat for discussions on the Berezinskii approach. This research has been supported by the National Science Centre (Poland) under Project No. 2016/21/B/ST2/01086 (J.J.) and 2019/35/B/ST2/00034 (J.Z.). We acknowledge support of the Foundation for Polish Science (FNP) through the first Polish-French Maria Sklodowska-Pierre Curie reward received by D. Delande and J. Zakrzewski. J. Janarek acknowledges also the support of French Embassy in Poland through the *Bourse du Gouvernement Français* program. We acknowledge the support of the PL-Grid structure which made numerical calculations possible.

[1] P. W. Anderson, Absence of diffusion in certain random lattices, Phys. Rev. **109**, 1492 (1958).

[2] G. Roati, C. D'Errico, L. Fallani, M. Fattori, C. Fort, M. Zaccanti, G. Modugno, M. Modugno, and M. Inguscio, Anderson localization of a non-interacting Bose-Einstein condensate, Nature (London) **453**, 895 (2008).

[3] J. Billy, V. Josse, Z. Zuo, A. Bernard, B. Hambrecht, P. Lugan, D. Clément, L. Sanchez-Palencia, P. Bouyer, and A. Aspect, Direct observation of Anderson localization of matter waves in a controlled disorder, Nature (London) **453**, 891 (2008).

[4] F. Jendrzejewski, K. Müller, J. Richard, A. Date, T. Plisson, P. Bouyer, A. Aspect, and V. Josse, Coherent Backscattering of Ultracold Atoms, Phys. Rev. Lett. **109**, 195302 (2012).

[5] I. Manai, J.-F. Clément, R. Chicireanu, C. Hainaut, J. C. Garreau, P. Szriftgiser, and D. Delande, Experimental Observation of Two-Dimensional Anderson Localization with the Atomic Kicked Rotor, Phys. Rev. Lett. **115**, 240603 (2015).

[6] G. Semeghini, M. Landini, P. Castilho, S. Roy, G. Spagnolli, A. Trenkwalder, M. Fattori, M. Inguscio, and G. Modugno, Measurement of the mobility edge for 3D Anderson localization, Nat. Phys. **11**, 554 (2015).

[7] H. Hu, A. Strybulevych, J. H. Page, S. E. Skipetrov, and B. A. van Tiggelen, Localization of ultrasound in a three-dimensional elastic network, Nat. Phys. **4**, 945 (2008),.

[8] A. A. Chabanov, M. Stoytchev, and A. Z. Genack, Statistical signatures of photon localization, Nature (London) **404**, 850 (2000).

[9] T. Schwartz, G. Bartal, S. Fishman, and M. Segev, Transport and Anderson localization in disordered two-dimensional photonic lattices, Nature (London) **446**, 52 (2007).

[10] T. Prat, D. Delande, and N. Cherroret, Quantum boomeranglike effect of wave packets in random media, Phys. Rev. A **99**, 023629 (2019).

[11] L. Tessieri, Z. Akdeniz, N. Cherroret, D. Delande, and P. Vignolo, Quantum boomerang effect: Beyond the standard Anderson model, Phys. Rev. A **103**, 063316 (2021).

[12] R. Sajjad, J. L. Tanlimco, H. Mas, A. Cao, E. Nolasco-Martinez, E. Q. Simmons, F. L. N. Santos, P. Vignolo, T. Macrì, and D. M. Weld, Observation of the Quantum Boomerang Effect, Phys. Rev. X **12**, 011035 (2022).

[13] Y.-J. Lin, K. Jiménez-García, and I. B. Spielman, Spin–orbit-coupled Bose–Einstein condensates, Nature (London) **471**, 83 (2011).

[14] C. Hamner, Y. Zhang, M. A. Khamehchi, M. J. Davis, and P. Engels, Spin-Orbit-Coupled Bose-Einstein Condensates in a One-Dimensional Optical Lattice, Phys. Rev. Lett. **114**, 070401 (2015).

[15] Y. Yue, C. A. R. Sá de Melo, and I. B. Spielman, Enhanced transport of spin-orbit-coupled Bose gases in disordered potentials, Phys. Rev. A **102**, 033325 (2020).

[16] In [12] it was shown that the initial state also has to be time-reversal invariant, a condition implicitly met by the initial states considered in [10] and in the present paper.

[17] F. Haake, S. Gnutzmann, and M. Kuś, *Quantum Signatures of Chaos*, Springer Series in Synergetics (Springer International, Cham, 2018).

[18] V. Oganesyan and D. A. Huse, Localization of interacting fermions at high temperature, Phys. Rev. B **75**, 155111 (2007).

[19] Y. Y. Atas, E. Bogomolny, O. Giraud, and G. Roux, Distribution of the Ratio of Consecutive Level Spacings in Random Matrix Ensembles, Phys. Rev. Lett. **110**, 084101 (2013).

[20] T. Prat, Ph.D. thesis, Université Pierre et Marie Curie, Paris, 2017, https://tel.archives-ouvertes.fr/tel-01687032.

[21] E. Akkermans and G. Montambaux, in *Mesoscopic Physics of Electrons and Photons* (Cambridge University Press, Cambridge, 2007), pp. 1–588.

[22] C. A. Müller and D. Delande, Disorder and interference: Localization phenomena, in *Ultracold Gases and Quantum Information, Lecture Notes of the Les Houches Summer School in Singapore* (Oxford University Press, Oxford, 2011), Vol. 91, pp. 441–533.

[23] See Supplemental Material at http://link.aps.org/supplemental/10.1103/PhysRevB.105.L180202 for the solution of the classical coupled Boltzmann equations, a sketch of the diagrammatic method used to compute the quantum boomerang effect in the absence of time-reversal invariance, the contributions of the various components to the center of mass position, and the dependence on the TRI breaking parameter Δ. It includes Ref. [36].

[24] H. Tal-Ezer and R. Kosloff, An accurate and efficient scheme for propagating the time dependent Schrödinger equation, J. Chem. Phys. **81**, 3967 (1984).

[25] C. Leforestier, R. Bisseling, C. Cerjan, M. Feit, R. Friesner, A. Guldberg, A. Hammerich, G. Jolicard, W. Karrlein, H.-D. Meyer, N. Lipkin, O. Roncero, and R. Kosloff, A comparison of different propagation schemes for the time dependent Schrödinger equation, J. Comput. Phys. **94**, 59 (1991).

[26] S. Roche and D. Mayou, Conductivity of Quasiperiodic Systems: A Numerical Study, Phys. Rev. Lett. **79**, 2518 (1997).

[27] A. Weiße, G. Wellein, A. Alvermann, and H. Fehske, The kernel polynomial method, Rev. Mod. Phys. **78**, 275 (2006).

[28] J. Janarek, D. Delande, N. Cherroret, and J. Zakrzewski, Quantum boomerang effect for interacting particles, Phys. Rev. A **102**, 013303 (2020).

[29] V. L. Berezinski, Kinetics of a quantum particle in a one-dimensional random potential (Kinetika kvantovoi chastitsy v odnomernom sluchainom potentsiale), Zh. Eksp. Teor. Fiz. **65**, 1251 (1973).

[30] A. Gogolin, Electron density distribution for localized states in a one-dimensional disordered system, Sov. J. Exp. Theor. Phys. **44**, 1003 (1976).

[31] E. Nakhmedov, V. Prigodin, and Y. Firsov, Localization dynamics in weakly disordered systems, Zh. Eksp. Teor. Fiz. **92**, 2133 (1987).

[32] J. P. R. Valdes and T. Wellens, Localization of wave packets in one-dimensional random potentials, Phys. Rev. A **93**, 063634 (2016).

[33] J. Janarek, T. Prat, D. Delande, and N. Cherroret (unpublished).

[34] G. A. Baker, *Essentials of Padé Approximants* (Academic Press, New York, 1975).

[35] F. Noronha and T. Macrì, Ubiquity of the quantum boomerang effect in localized systems, arXiv:2203.16719.

[36] M. Abramowitz and I. A. Stegun, *Handbook of Mathematical Functions* (National Bureau of Standards, Washington, DC, 1966).